International Journal of GEOMATE, June., 2021, Vol.20, Issue 82, pp.101-108
ISSN: 2186-2982 (P), 2186-2990 (O), Japan, DOI: https://doi.org/10.21660/2021.82.6035
Geotechnique, Construction Materials and Environment

DYNAMIC PROPERTIES OF POST-BUCKLED SHAPE MEMORY ALLOY AND ITS APPLICATION TO A BASE ISOLATOR FOR VERTICAL VIBRATION

Atsushi Urakawa [1], *Takumi Sasaki [2] and Hiroki Cho [3]

[1] Graduate school of Environmental Engineering, The University of Kitakyushu, Japan;
[2,3] Faculty of Environmental Engineering, The University of Kitakyushu, Japan

*Corresponding Author, Received: 15 Jan. 2021, Revised: 21 Feb. 2021, Accepted: 07 Mar. 2021

ABSTRACT: In recent years, high performance and compact vibration isolators have been in demand to support the advancement of precision technology. Among various vibration isolators, a passive vibration isolator is the most commonly adopted form due to its simplicity, stability and low cost. Previously, the authors have proposed a simple and compact passive vibration isolator for the vertical direction using a post-buckled shape memory alloy (SMA) beam. This isolator achieved a low natural frequency assuring high static stiffness by utilizing the negative tangent stiffness of a post-buckled SMA beam. It is expected that the appearance of the negative stiffness is related to the phase transformation of a post-buckled SMA beam, however, the fundamental principle of the appearance and the response for a reciprocating motion (vibration) have not been clarified. In this study, to clarify these characteristics, the restoring force of an SMA beam subjected to reciprocating motion in its post-buckled state was measured experimentally and predicted by Finite Element Analysis in which the phase transformation of the post-buckled SMA was considered. As the result, it was found that the restoring force converged to a certain force when SMA was subjected to reciprocating motion. It was also found that the negative tangent stiffness arose when the phase of SMA transforms from Austenite phase to Martensite phase in compression process. Therefore, SMA with small hysteretic property in the stress-strain curve is appropriate for an effective isolation element. In future research, it will be necessary to validate the performance of the isolator considering the phase transformation.

Keywords: Buckling, Shape memory alloy, Base isolation, Passive isolation, Nonlinear isolator

1. INTRODUCTION

Base isolation for precision equipment, for example, precision sensors and precision processing machinery, is a crucial technology for assuring their performance and reliability. Also, isolation technology for vibration and sound noise reduction of vehicles have become increasingly important due to pursuit of their comfort and quietness [1-3]. In base isolation technology, passive vibration isolators are the most commonly adopted form due to their simplicity, stability and low cost. Their effectiveness, in terms of, isolation performance and isolation frequency bandwidth, relies on being able to achieve a low natural frequency when supporting an isolated object. Low natural frequency can be achieved by supporting an isolated object with a soft spring element. However, when they were applied to isolation in the vertical direction, low stiffness can result in impractically large static deflection due to the weight of the isolated object. Consequently, a key trade-off in the selection of a spring element for an isolator for vertical direction is their low dynamic stiffness, which governs the effectiveness of an isolator, versus their high static stiffness, which is needed for static load bearing capacity. These conflicting requirements can in principle be realized by adopting a nonlinear isolator that exhibits high stiffness for a static force and low stiffness for a dynamic force. One of the devices with such a nonlinear characteristic can be realized by inserting in parallel with the main load bearing isolator element a snap-through mechanism with negative stiffness. Examples in the literature include spring lever mechanisms [4-7], bi-stable plates [8] and magnets [9]. An alternative approach is making use of the nonlinear restoring force of a post-buckled beam that maintains much of its static stiffness in its buckled state but whose tangent stiffness dramatically reduces [10-14]. In the process of the investigation for dynamic properties of post-buckled elements, the authors have detected the negative tangent stiffness characteristic of a post-buckled plate-shaped Titanium-Nickel based shape memory alloy beam (hereafter, called SMA beam) in the previous study [15]. The authors have also proposed a passive vibration isolator using a post-buckled SMA beam and investigated its isolation performance experimentally. In that study, the isolator achieved a low natural frequency of about 3 Hz and exhibited considerable isolation performance. However, few studies have examined the static and dynamic properties of the restoring force of a post-buckled SMA. Especially, the expression principle of the negative tangent stiffness, the restoring force of a post-buckled SMA for reciprocating motion and the dynamic characteristic of a post-buckled SMA have not been clarified although they are important for designing and predicting the performance of an isolator.

The motivation for this study is to clarify experimentally and numerically the fundamental characteristic of a post-buckled SMA beam which is needed for establishing the design guideline for an isolator using a post-buckled SMA beam. In this paper, we focused on the following characteristics; (1)The response of a post-buckled SMA for reciprocating motion is experimentally and numerically investigated and their properties are compared qualitatively. (2)The expression principle of the negative stiffness is investigated numerically focusing on the phase transformation of a post-buckled SMA beam.

In section 2, a general overview of a passive isolator, the restoring force of a post-buckled SMA beam and the conceptual design of a passive vibration isolator for vertical direction using a post-buckled SMA beam are described. In section 3, the restoring force of a post-buckled SMA beam for several reciprocating conditions is described. Section 4 describes the numerical investigation for the restoring force of a post-buckled SMA beam, which was obtained by FE analysis considering the phase transformation of SMA material, and compared with the experimental results qualitatively.

2. OVERVIEW OF A PASSIVE VIBRATION ISOLATOR AND AN ISOLATOR USING A POST-BUCKLED SMA BEAM

2.1 Overview of a Passive Vibration Isolator

The most fundamental model of a passive vibration isolator for the vertical direction is shown in Fig. 1. An isolated mass m is supported by a linear spring of which spring constant is k and a linear dashpot of which viscous damping coefficient is c and vertical oscillation is imposed from the base. The undamped natural frequency of the system is given as follows.

$$\omega_n = \sqrt{\frac{k}{m}} \tag{1}$$

Considering the frequency response of the vibration transmissibility between an isolated mass and base, the effectiveness of the isolator relies on being able to achieve a low natural frequency. However, low stiffness, which realizes a low natural frequency, can result in impractically large static deflection due to the weight of the isolated object. This dilemma can in principle be solved by adopting a nonlinear isolator that exhibits high stiffness when loaded statically and low stiffness in relation to small oscillations about the static equilibrium position. One of the techniques to realize such nonlinearity is making use of the nonlinear restoring force of a post-buckled beam.

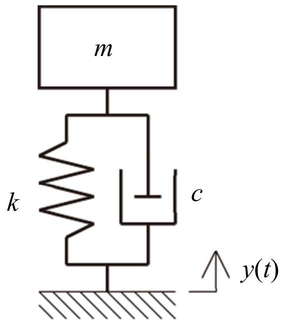

Fig.1 The most fundamental model of a passive vibration isolator for the vertical direction

2.2 Conceptual Design of an Isolator Using SMA

Authors have reported that the static restoring force of the SMA beam, which is subjected to compressive external displacement at both ends of the beam for longitudinal direction, exhibits the negative tangent stiffness in its post-buckled state. Figure 2 shows a buckled SMA beam when longitudinal compressive displacement was imposed at the end of the beam. An exsample of measured static restoring force of a post-buckled SMA beam is shown in Fig. 3. As shown in the figure, the static restoring force decreases by increasing the imposed compressive displacement, that is, SMA exhibits the negative tangent stiffness characteristic. By utilizing this characteristic, the authors have proposed a vibration isolator using a post-buckled SMA beam. The conceptual diagram of an isolator is shown in Fig. 4. This isolator incorporated a post-buckled SMA beam, a coil spring and constraint elements that constrained the motion of the isolated object except for the vertical motion. The SMA beam is oriented vertically. One end is fixed to a base and the weight of the isolated object is acting at the other end. If the weight of the isolated object is larger than the buckling load of the SMA beam, the SMA beam will buckle. Then, if the spring constant of a coil spring, which is installed in parallel to the post-buckled beam, was chosen so as only just to cancels the negative tangent stiffness of the post-buckled SMA beam, in principle, quasi-zero-stiffness (QZS) will be achieved and ideal isolation would be realized.

For designing and predicting the performance of this isolator the static and dynamic properties of a post-buckled SMA beam are the essential properties. However, studies for these properties are insufficient so far. Then, in the following sections, the restoring force of SMA beam simulating the deflection when it is used for the isolator are examined experimentally and numerically.

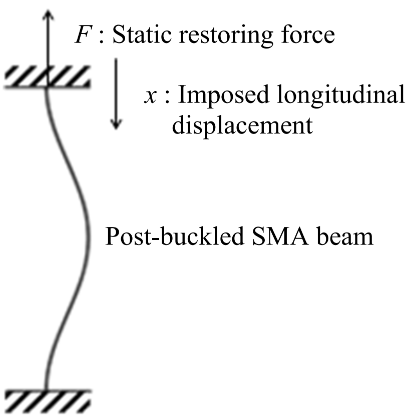

Fig.2 Schematic diagram of a post-buckled SMA beam

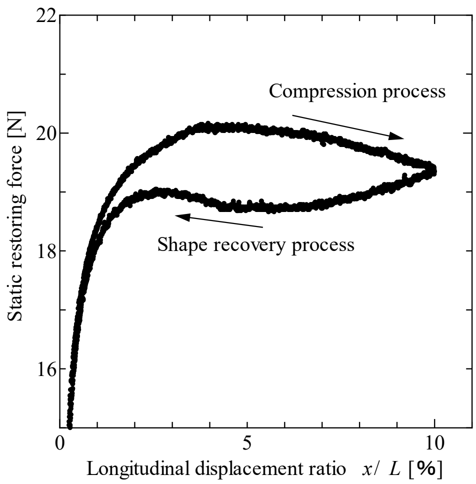

Fig.3 Static restoring force of a post-buckled SMA beam

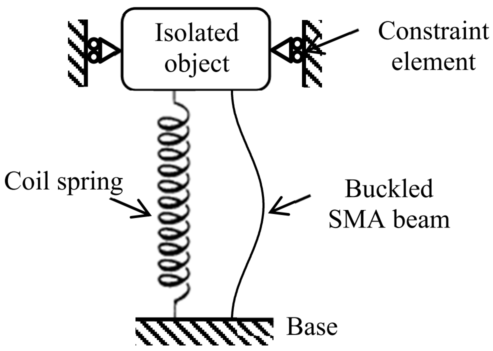

Fig.4 Conceptual diagram of a vibration isolator using a post-buckled SMA beam

3. EXPERIMENTAL INVESTIGATION

In order to apply a post-buckled SMA beam to a vibration isolator, it is necessary to examine the restoring force properties of a post-buckled SMA beam when it is subjected to vibrational motion. In this section, the restoring force of a post-buckled SMA beam when it is subjected to reciprocal motion is examined experimentally.

3.1 Experimental Setup

A schematic view of the experimental setup is shown in Fig. 5. Ti-Ni based SMA beam, with specifications summarized in Table 1, was used. Both ends of the SMA beam were clamped by stainless steel plate. One end was fixed to the base rigidly. Another end was supported by the linear guide, which corresponds to a constraint element, and the linear guide was mounted on the linear slider, which corresponds to a device for imposing longitudinal external displacement. The restoring force of the SMA beam for the longitudinal direction was measured by the load cell. Since the moving speed of the linear slider was controlled to sufficiently slow (0.1mm/s), the quasi-static restoring force was measured. Stainless plates at both ends had electrodes and the SMA beam could be heated by Joule heat of itself by applying electric current directly to the SMA beam. The temperature of the SMA beams was monitored by a thermocouple set at the middle of the SMA beam (omitted in Fig. 5) and kept to 30°C by controlling the electric current with a PID control system.

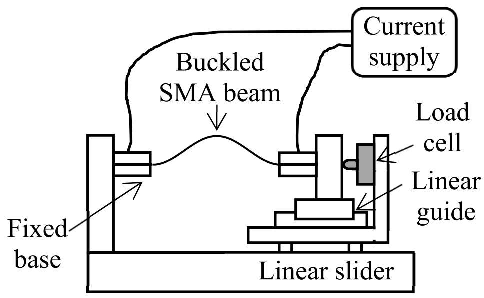

Fig.5 Schematic view of the experimental setup

Table 1 Specification of SMA used in the experiment

Material composition	Titanium-50.2at%Nickel	
Heat treatment condition	Temperature	753 [K]
	Time	40 [min]
	Cooling condition	Air cooling
Dimension	Width	5.5 [mm]
	Thickness	0.5 [mm]
	Length	110 [mm]

3.2 Restoring Force of a Post-Buckled SMA

In order to simulate the restoring force of the post-buckled SMA beam when it was used as a base isolation system, the following experiment was conducted.

Experiment 1: impose 9mm longitudinal displacement in order to make the SMA beam buckle, and subsequently impose 10 times reciprocating displacement of which amplitude was increased by 0.2mm per one reciprocation. After the reciprocation, imposed displacement was recovered to the original position (0mm). By this experiment, the restoring force behavior of the post-buckled SMA beam when the amplitude of an isolated object was varied could be measured.

Experiment 2: impose 10mm longitudinal displacement firstly, and subsequently, let the displacement recover to a certain displacement ((a)3mm, (b)4mm or (c)5mm), and finally impose 500 times reciprocating displacement of which amplitude was 1mm. After the reciprocation, imposed displacement was recovered to the original position (0mm). By this experiment, the restoring force behavior of the post-buckled SMA beam when it had been subjected to large deflection could be measured.

The solid line in Fig. 6(a) shows the measured restoring force for Experiment 1. The dashed line in the figure shows the restoring force for one-time reciprocation for comparison. Fig. 6(b) is the magnification of Fig. 6(a). It is confirmed from the experiment 1 that the magnitude of restoring force drops drawing a hysteretic loop while the reciprocating motion(Fig. 5 and Fig. 6). Also, it is confirmed that the magnitude of the hysteretic loop gets larger when the large amplitude was imposed.

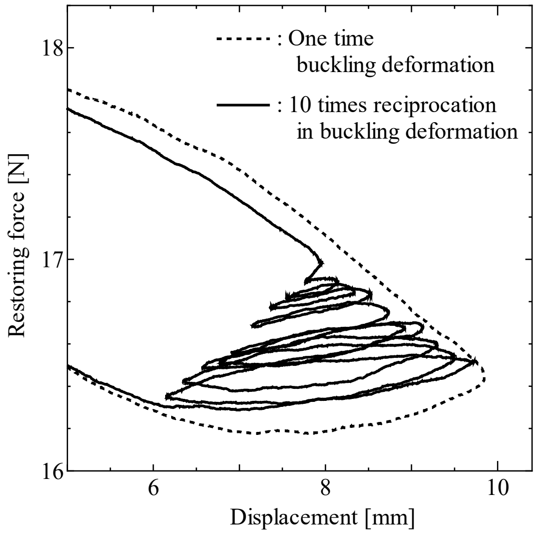

Fig.6(b) Magnification of Fig. 6(a)

The lower limit of the dropping restoring force will be considered in the following section(Fig. 6).

The solid lines and dashed lines in Fig. 7 show the measured restoring force for Experiment 2 and the approximate line when the restoring forces in the reciprocating process were approximated by the linear function. The experiment confirmed that the restoring force in reciprocating motion differed depending on the displacement recovery condition (start point of reciprocating motion), while the restoring force in the whole process except in reciprocal process was almost the same(Fig. 7). The gradient of the dashed line corresponds to the approximative tangent stiffness in reciprocating motion and that of shape recover condition (a)3mm, (b)4mm and (c)5mm was 0.175 N/mm, 0.132 N/mm and 0.105 N/mm, respectively.

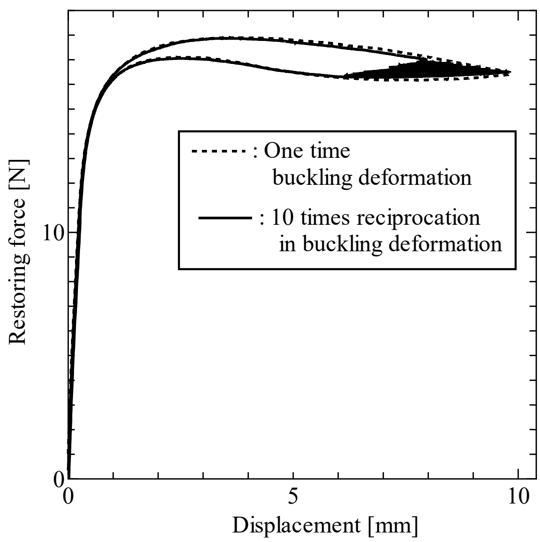

Fig.6(a) Measured restoring force of the post-buckled SMA beam in reciprocating motion (Experiment 1)

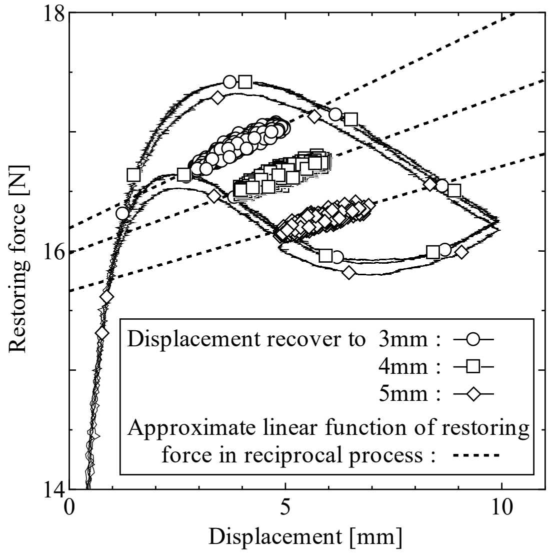

Fig.7 Measured restoring force of the post-bucked SMA beam in reciprocating motion and approximate linear function (Experiment 2)

This result indicates that the approximative tangent stiffness also differed depending on the start point of reciprocating motion and it didn't exhibit the negative tangent stiffness but the positive tangent stiffness. These properties, the restoring force and the tangent stiffness vary depending on reciprocation condition, are considered not to be appropriate for the use for an isolator, because this means that the isolation performance varies depending on the vibration condition. The countermeasure to overcome these unfavorable properties will be investigated in the later section.

4. NUMERICAL INVESTIGATION

In this section, the post-buckled properties of an SMA beam are numerically investigated. On the numerical analysis, Finite Element Analysis was conducted by using ANSYS 19.0.

4.1 Analytical Model

On the numerical analysis, the SMA beam of which dimension was 7.2mm in width, 50mm in length and 0.43mm in thickness was used. Both ends of the beam were rigidly fixed except the degree of freedom for longitudinal direction at one end was set free. The material properties (stress-strain curve) of SMA were approximated by a piecewise linear property composed of four linear lines as shown by the solid line in Fig.8. The SMA beam was modeled by using three-dimensional laminated solid-shell elements in order to figure out accurately the stress and the phase transformation of the inner part of SMA material.

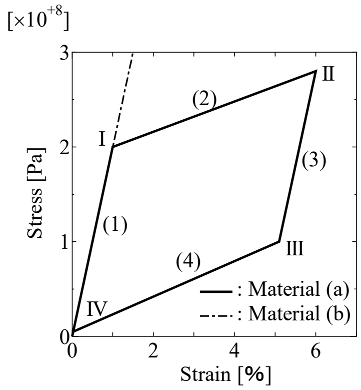

Fig.8 Stress-strain curve used in the numerical analysis

4.2 Effect of Phase Transformation of SMA on Negative Tangent Stiffness

The effect of phase transformation of the SMA beam on the development of the negative tangent stiffness in its post-buckled state was investigated. In this analysis, two types of material, with specifications summarized in Table 2, were used, where σ_1, σ_2, σ_3 and σ_4 of material (a) represent the stress at the intersection point of linear lines at I, II, III and IV of fig.8, respectively. E, ε and ν represent the gradient of the line (1), the difference of strain between intersection points of I and II, and III and IV and Poisson's ratio, respectively. The deformation process on the line (1) can be regarded as the deformation process of the austenite phase, and that on the line (2) is the deformation process of phase transformation from the austenite phase to the martensite phase. Also, the deformation process on the line (3) can be regarded as the elastic deformation of the martensite phase, and that on the line (4) is the deformation process of phase transformation from the martensite phase to the austenite phase. Material (a) approximates a material properties of Ti-Ni based SMA, while material (b) is the material of which phase transformation is suppressed by setting sufficiently large stress for σ_1.

The force-displacement curve of the post-buckled beam when 5mm displacement was imposed for longitudinal direction is shown in Fig. 9. Imposed displacement (horizontal axis) and restoring force (primary vertical axis) are normalized by the length of the beam and the buckling load obtained from the linear buckling theorem, respectively. The solid line and the dashed line show the restoring force of materials (a) and (b). Open circles and open triangles in Fig. 9 show the volume fraction of the martensite phase in the compression process of material (a) and (b), respectively, by the secondary vertical axis. The analytical result in Fig. 9 indicates that the restoring force of material (a) exhibits negative tangent stiffness in the displacement range beyond 4% in the compression process and within 4% in the shape recovery process. Also, in the compression process of material (a), the negative tangent stiffness appears as phase transformation from the austenite phase to the martensite phase proceeded, while the restoring force of material (b) exhibits positive stiffness in all displacement range in the figure and it exhibits no phase transformation. These results confirmed that the development of the negative tangent stiffness is caused by the phase transformation of the SMA beam.

Table 2 Specification of SMA material used in the numerical analysis

Material (a)	Material (b)
$\sigma_1 = 200$ [MPa]	$\sigma_1 = 2000$ [MPa]
$\sigma_2 = 280$ [MPa]	$\sigma_2 = 2800$ [MPa]
$\sigma_3 = 100$ [MPa]	$\sigma_3 = 1000$ [MPa]
$\sigma_4 = 5$ [MPa]	$\sigma_4 = 50$ [MPa]
$E = 20$ [GPa], $\varepsilon = 0.05$, $\nu = 0.3$	

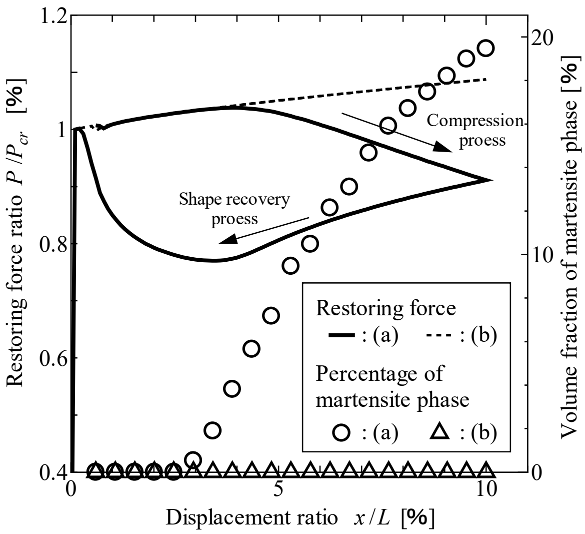

Fig.9 Force displacement curve and volume fraction of the martensite phase

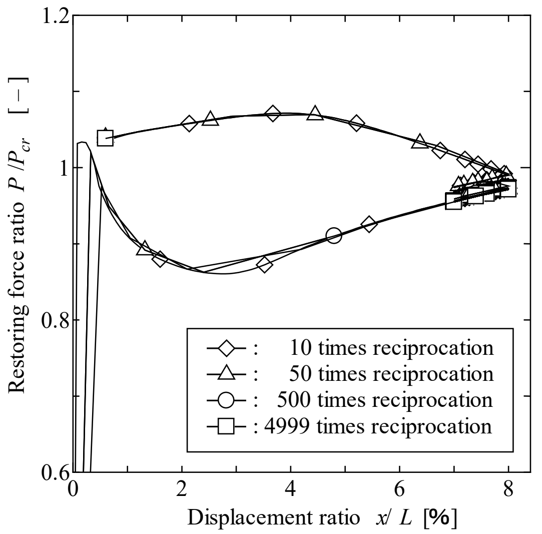

Fig.10 Restoring force of the beam in reciprocating motion (Analysis 1)

4.3 Restoring Force in Reciprocating Motion

In order to investigate the restoring force of a post-buckled SMA beam in reciprocation motion, the following analysis was conducted.
Analysis 1: impose 4mm longitudinal displacement in order to make the SMA beam buckle, and subsequently impose reciprocating displacement of which amplitude was 0.25 mm for (a)10 times, (b)50 times, (c)100 times and (d)4999 times. After the reciprocation, imposed displacement was recovered to the original position (0mm).
Analysis 2: impose 4mm longitudinal displacement firstly, and subsequently let the displacement recover to 0.8mm, and subsequently impose reciprocating displacement of which amplitude was 0.5mm for 500 times. After the reciprocation, imposed displacement was recovered to the original position (0mm).
Material (a) in table 2 was used for the analysis.

The restoring force obtained for Analysis 1 (Fig. 10 and Fig. 11) confirmed that the magnitude of restoring force drops while the reciprocating motion was imposed. This characteristic is qualitatively coincide with the result of experiment 1. Also, if the number of reciprocating time was increased more than 5000 times, it will not lower than that of 4999 times.

The restoring force obtained for Analysis 2 (Fig.12) confirmed that the magnitude of restoring force rises while the reciprocating motion. Also, if the number of reciprocating time was increased more than 501 times, it will not rise than that of 500 times.

These results confirmed that the magnitude of restoring force drops or rises while the reciprocating motion was imposed in the compression process or shape recovery process, respectively, and converges to a certain force. This phenomenon qualitatively

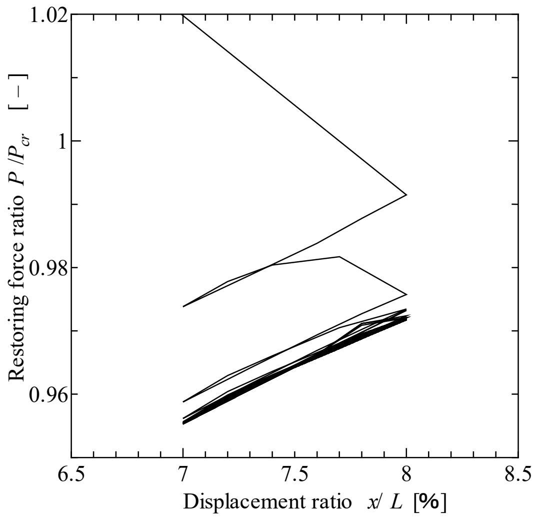

Fig.11 Magnification of Fig. 10 at reciprocating condition (d)

corresponds to the experimental result referred to in the last section. The restoring force in Fig.10 doesn't draw a hysteretic loop, which is different from the experimental result, however this is because that the reciprocating amplitude of numerical analysis was smaller than the experiment and the stress-strain curve was approximated by piecewise lines.

4.4 Desired Specification of SMA for an Isolator

The restoring force characteristics referred to in previous sections were not appropriate for a high performance isolator due to positive stiffness characteristics in the reciprocating motion. The appearance of positive stiffness is thought to be the most likely cause of the gradient of the stress-strain curve in the shape recovery process, that is, the gradient of the line (3) in fig. 8. One of the options

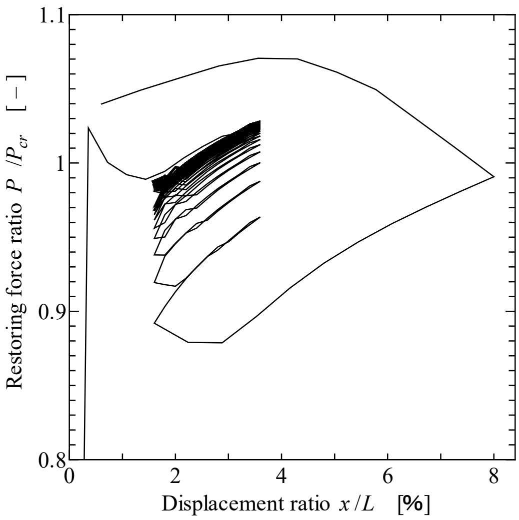

Fig.12 Restoring force in reciprocating motion in shape recovery process (Analysis 2)

Table 3 Specification of a material of which hysteresis in stress-strain curve is small

Material (c)
$\sigma_1 = 200$ [MPa] , $\sigma_2 = 280$ [MPa],
$\sigma_3 = 275$ [MPa] , $\sigma_4 = 195$ [MPa]
$E = 20$ [GPa], $\varepsilon = 0.05$, $\nu = 0.3$

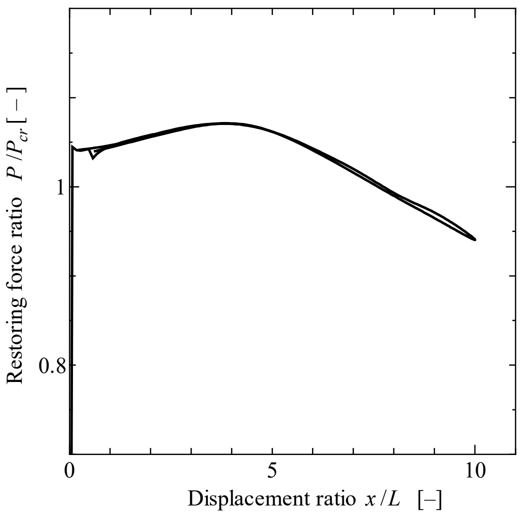

Fig.13 Restoring force of the beam with small hysteretic material

to mitigate the effect of the gradient of the line (3) is using a material of which stress-strain curve has small hysteretic property. An example of such material properties is summarized in table 3. The restoring force of the beam with material (c) (Fig. 13) exhibits negative tangent stiffness in the displacement range beyond 4% and almost constant tangent stiffness could be obtained in the displacement range beyond 5% even in the compression process or in the shape recovery process. This kind of property (small hysteretic property of the stress-strain curve) is appropriate for the system shown in Fig. 3 since desired isolation performance would be obtained regardless of vibration condition. It is known that Copper based SMA exhibits small hysteretic property, so the experimental investigation for dynamic properties of a post-buckled Copper based SMA beam is desired in future work.

5. CONCLUSION

This paper has investigated the dynamic properties of a post-buckled SMA beam experimentally and numerically. The restoring force of Titanium-Nickel based SMA beam exhibited negative tangent stiffness for one-time buckling deformation, however, it exhibited positive stiffness when the reciprocal motion was imposed in the post-buckled state. The restoring force varied while in reciprocation and converged at a certain force. The restoring force of a beam with a small hysteretic material exhibit almost constant tangent stiffness in a displacement range beyond 5%. For a high performance passive isolator, experimental investigation for the dynamic properties of SMA material which has small hysteretic property needs to be addressed in future studies.

6. ACKNOWLEDGMENTS

This work was supported by JSPS Grant-in-Aid for Scientific Research (C) number 18K04025.

7. REFERENCES

[1] Boonthum Wongchai, Poranat Visuwan, Sathaporn Chuepeng, Time and frequency analysis of the engine support vibration with hydrogen-diesel dual-fueling, International Journal of GEOMATE, Vol. 16, Issue 56, pp. 1-8

[2] Suphattharachai Chomphan and Boonthum Wongchai, Correlation analysis of vibration and sound signals of a gasoline-engine car, International Journal of GEOMATE, Vol. 18, Issue 67, pp. 195-201

[3] Suphattarachai Chomphan, An analysis of vibration for a gasoline-engine car driving on three types of roads, International Journal of GEOMATE, Vol. 20, Issue 80, pp. 29-35

[4] Park, S. T. and Luu, T. T., Techniques for Optimizing Parameters of Negative Stiffness, Proc of IMechE, Journal of Mechanical Engineering Science, Vol. 221, 2007, pp. 505-511.

[5] Xingtian Liu, Xiuchang Huang, Hongxing Hua, On the characteristics of a quasi-zero stiffness isolator using Euler buckled beam as negative

stiffness corrector, Journal of Sound and Vibration, 332(14), 2013, pp. 3359-3376.

[6] Le, T., Ahn, K.K., A vibration isolation system in low frequency excitation region using negative stiffness structure for vehicle seat, Journal of Sound and Vibration, 330(26), 2011, pp. 6311-6335.

[7] Araki, Y., Asai, T., Kimura, K,, Maezawa, K., Masui, T., Nonlinear vibration isolator with adjustable restoring force, Journal of Sound and Vibration, 332(23), 2013, pp. 6063-6077.

[8] Shaw, AD, Neild, SA, Wagg, DJ, Weaver, PM & Carrella, A, A nonlinear spring mechanism incorporating a bistable composite plate for vibration isolation, Journal of Sound and Vibration, 332(24), 2013, pp. 6265-6275.

[9] Carrella, A., Brennan, M.J., Waters, T.P. and Shin, K., On the design of a high-static-low-dynamic stiffness isolator using linear mechanical springs and magnets, Journal of Sound and Vibration, 315(3) 2008, pp. 712-720.

[10] Winterflood, J., Blair, D. G. and Slagmolen, B., High Performance Vibration Isolation using Springs in Euler Column Buckling Mode, Physics Letters A, Vol. 300,2002, pp. 122-130.

[11] Tsuji, Y., Sasaki, T., Waters, T.P., Fujito, K. and Wang, D., A Nonlinear Vibration Isolator Based on a Post-buckled Inverted L-shaped Beam, The Sixth World Conference on Structural Control and Monitoring,2014, Barcelona.

[12] Sasaki T., Waters T.P. and Tsuji Y., Experimental study on a nonlinear vibration isolator on a post-buckled inverted L-shaped beam, Mechanical Engineering Journal, Vol.2, No.3, 2015, pp.1-11.

[13] Sasaki T., Waters T. P., Analysis of a vibration isolation table comprising post-buckled Γ-shaped beam isolators, Journal of Physics: Conference series, Vol. 744, 2016, No. 1: 1-8.

[14] Chiyojima T. and Sasaki T., Development of a passive vibration isolator using a post-buckled Γ-shaped beam (Improvement of the isolation performance by considering mode shapes of a Γ-shaped beam), Proc. of Asia Pacific Vibration Conference 2017, 2017, pp. 11-16.

[15] Sasaki T. and Kimura Y., Experimental Study on a Passive Vibration Isolator Utilizing Dynamic Characteristics of a Post-Buckled Shape Memory Alloy, Proc. of Asia Pacific Vibration Conference 2019, 2019, pp. 1-6.